J Mater Sci (2007) 42:4485–4493
DOI 10.1007/s10853-006-0457-1

Relationship between thermal and sliding wear behavior of Al6061/Al_2O_3 metal matrix composites

Serdar Osman Yılmaz · Soner Buytoz

Received: 12 October 2005 / Accepted: 15 May 2006 / Published online: 15 February 2007

Abstract Al6061 alloy and Al6061/Al_2O_3 metal matrix composites (MMCs) were fabricated by stir casting. The MMCs were prepared by addition of 5, 10 and 15 wt% Al_2O_3 particulates and the size of particulates was taken as 16 μm. The effect of Al_2O_3 particulate content, thermal properties and stir casting parameters on the dry sliding wear resistance of MMCs were investigated under 50–350 N loads. The dry sliding wear tests were performed to investigate the wear behavior of MMCs against a steel counterface (DIN 5401) in a block-on-ring apparatus. The wear tests were carried out in an incremental manner, i.e., 300 m per increment and 3,000 m in total. It was observed that, the increase in Al_2O_3 vol% decreased both thermal conductivity and friction coefficient and hence increased the transition load and transition temperature for mild to severe wear during dry sliding wear test.

Introduction

Metal matrix composites (MMCs) have higher specific modulus, strength [1], and wear resistance [2–4] than conventional alloys. Hence, MMCs are alternative to conventional materials in a number of specialized application areas [6]. There are a lot of studies on the effect of the contact load on the wear resistance of various MMCs under dry sliding conditions. In these studies it was indicated that the composite wear rates were more than one order of magnitude lower than those of the unreinforced counterparts at low contact pressures. The better composite wear resistance was rationalized in terms of the higher load-bearing capacity of the ceramic particles, which limited the amount of plastic deformation in the matrix. Moreover, during the wear process, hard particulates affect the steel counterbodies, and a thin layer of oxidized iron formed and acted as a solid lubricant. For this reason, the wear rate and friction coefficient is reduced. On the other hand, the elevated contact pressure is high enough to fracture the particulates near the contact surface, therefore the particulates no longer acts as load-bearing elements, and the wear rate was controlled by the matrix.

Metal matrix composites (MMCs) have advantages for engineering materials [4]. The MMCs are especially reinforced with fibers, whiskers, or particulates [5]. Al based MMCs have improved strength, high modulus and wear resistance over conventional Al alloys. The properties of discontinuous Al-MMC make them attractive for wear resistance materials [6]. MMCs are fabricated by addition of a reinforcement phase to the matrix by one of the following techniques: powder metallurgy processing [7]; spray atomization and co-deposition [8]; plasma spraying [9]; stir casting (compo-casting) [10]; and squeeze casting [11]. The stir casting process is the most economical process among these processes. However, it has some restrictions due to density of the reinforced phases. Hence, the volume fraction and the size of the reinforcements are limited. Several factors influence the quality of the MMCs; one of the most important factors is the metal melt's metal ability to wet the ceramic particulates [12]. MMCs are common due to availability, low cost,

S. O. Yılmaz (✉) · S. Buytoz
Department of Metallurgical Engineering, Fırat University, 23119 Elazığ, Turkey
e-mail: osyilmaz@firat.edu.tr

independence of mechanical properties from particulate orientation [13] and production [10–13]. The MMCs have been made either by adding particulates externally [14] or by manipulating solidification [15, 16] to result in particulates embedded in a matrix. In addition, there are two types of foundry methods for making composites with externally added particulates, depending on the temperature at which the particulates are introduced in the melt. In liquid metallurgy process [14] the particulates are added above the liquidus temperature of the molten alloy.

In the soft matrix alloys, the wear rates decrease with increasing reinforcement volume fraction [17]. On the other hand, the strength of MMCs reduced with porosity content [18]. Thus, the interrelation of process variables in vortex method and the resulting porosity content is important. The stir casting composites usually contain inherent porosity, and the degree of the porosity depends on the pouring temperature and the volume fraction of the reinforcements [19].

The temperature affects the wear rate, and especially after a critical temperature the wear mechanism changes with a transition from mild to severe wear in MMCs [20]. The hard reinforcements and load are effective on transition temperature; reinforcers reduce the wear rate in the mild wear regime and increase the transition temperature. However, they did not provide any substantial benefit above the transition temperature, and the transition temperature decrease as the contact load increases [21].

In some investigation it was noted that the effect of the hard particulates on the thermal conductivity of samples changes as function of temperature. Nevertheless, the thermal conductivity increases in a polynomial function through the entire temperature change during wear. The change of transition temperature seems to be controlled by the reduction in the matrix mechanical properties with the temperature. The thermal stability in the matrix provided by the presence of carbides and intermetallic phases are thus responsible for the higher transition temperature [22, 23]. The role of the carbides on the transition to severe wear can be attributed to the critical transition temperature concept.

The aim of this research was to investigate the influence of temperatures on the dry sliding wear behavior of Al6061/Al_2O_3 MMCs, to evaluate the effect of porosity, as well as the volume fraction of Al_2O_3 particulates on the dry sliding wear property of stir casting, in addition to designate the relationship between the wear mechanisms, stir casting parameters and thermal properties of the materials.

Materials and experimental techniques

The chemical compositions and physical characteristics of the samples and Al_2O_3 particulates are given in Tables 1 and 2, respectively. Composites containing Al_2O_3 reinforcement with an average particulate size of about 16 μm were prepared by a stir casting process. A graphite crucible having an arrangement for bottom pouring is heated inside a resistance heating muffle furnace. About 500 g of aluminum alloy is melted in the crucible heated to 975 °C. The melt is allowed to cool and the particulate additions are performed at desired temperature. When the temperature of the melt is 20–30 °C above the pouring temperature, preheated stirrer is introduced in the melt. Agitation of the melt is started at the desired speed as 10 rev/min. and the particulates are introduced in the vortex in the ratio of 5, 10 and 15 vol%. The stirring is continued to prepare homogenous slurry. As pouring temperature, different temperatures between 850 °C and 910 °C were applied. The slurry is cast into a permanent steel mould of size 25 × 30 × 300 mm, by removing the graphite stopper from the bottom of the crucible. The slurry was poured into preheated die cavity (275 °C). The preheated ram attached to hydraulic press, which was used to maintain 50 MPa pressure during solidification. This pressure is maintained for 40 s. After casting, for determination of the effect of the homogenization on the microhardness and microstructure of the samples, 450 °C, 30 min homogenization heat treatment was applied to both Al6061 alloy and Al6061/Al_2O_3 MMCs.

Samples for microscopic examination were prepared by standard metallographic procedures; they were then etched with Keller reagent and examined by optical and scanning electron microscopy. For detection of the effect of porosity on the dry sliding wear property, different pouring temperatures were used ranging from 850 °C to 910 °C to prepare the samples having 5–15 vol% Al_2O_3.

Table 1 Chemical composition of the Al6061 alloy and Al_2O_3 powders

Al6061 alloy	Cu	Fe	Mg	Si	Cr	Zn	Al
wt%	0.25	0.6	0.86	0.56	0.02	0.05	Balance
Al_2O_3	Al_2O_3	Cr_2O_3	FeO	TiO_2			
wt%	99.435	0.015	0.38	0.17			

Table 2 Physical characteristics of the samples and Al_2O_3 reinforcement

Sample number	Al6061 alloy amount (vol%)	Apparent density "D_{mes}" (g cm^{-3})	Theoretical density "D_{mes}" (g cm^{-3})	Shape
S1	95	1.63	2.60	Irregular
S2	90	1.69	2.71	
S3	85	1.72	2.73	
Al_2O_3 reinforcements (16 μm)	–	1.69	2.71	Irregular

Hence, the relative amounts of each of these constituents are to be determined for a quantitative correlation of properties with relative amounts of constituents. The particulates can be embedded deep inside the pores; hence, quantitative metallography may not be accurate for determining relative amounts of porosities by point counting. Therefore, density measurements are used with the results of quantitative metallography to obtain the volume fraction of porosities [23].

Specimens in the form of 20 × 10 × 5 mm rectangular pieces were cut and polished to 600 grit finishes. Wear tests were carried out on a block-on-ring tester. Tempered sliding rings (DIN 5401, hardness 797 HV) of 45 mm in diameter were used as counterbodies. They were gripped to avoid rolling during the test. All of the tests were carried out five times with a normal force of 50–350 N on the sliding ring, and at a sliding speed of 0.3 m/s. Temperature was modified between 300 K and 475 K, and the weight loss was measured by using an electronic balance with a resolution of 0.01 mg. Wear losses was obtained by determining the masses of the samples before and after wear tests. The wear rates were calculated by converting the mass loss measurements (to the nearest 0.1 mg) to volume loss by using the respective densities.

Microstructures of specimens were investigated with scanning electron microscopy (SEM), energy-dispersive spectrometry (EDS). The electrical resistivity of the samples were measured by using two probe methods at a temperature range between 260 K and 370 K, by applying a DC voltage.

Results

Microstructure

Al6061 alloy and Al6061/Al_2O_3 MMCs were produced by stir casting. The close control system was used during all treatments. The microstructure of the Al6061 show that the solid structure of the Al6061 contains the α-AlFeSi and probably Mg_2Si phases which is so small that could not be detected by SEM. The structure having this morphology demonstrates the best mechanical properties, because the Mg_2Si phase has low mechanical values [24]. Before reinforcement of Al6061 matrix with Al_2O_3 particulates, it was aimed to determine the cooling rate for the formation of the most appropriate morphology of Al6061. Depending on cooling rates, it was known that the microstructure of the Al6061 alloy samples crystallizes in distinctly different morphologies as (β-phase), and (α-phase) [25, 26]. At very low cooling rates (≈0.5 °C/s), the α-phase begins to crystallize as primary-α crystals (Fig. 1a). The increase of cooling rate (≈10 °C/s) shows that the α-phase is constrained to interdendritic areas and lead to crystallization in the form of α-phase (Fig. 1b). Most of the iron compound crystallized in the form of β-phase at very high cooling rates (≈20 °C/s). The superheating is even effective on microstructure. It was seen that AlFeSi phases crystallized in the needlelike form (β-phase) for all cooling rates at a low superheating temperature of 750 °C. On the other hand, crystallization occurred in the form of (α–β) phase mixture at high superheating temperatures of 900 °C. The investigations have show that in the microstructures of the Al6061 having Al_2O_3 particulates, the presence of Al_2O_3 particulates act as nucleation sites for formation of β-phase (Fig. 1c). It is considered that due to the activation of Al_2O_3 nuclei particulates, the formation temperature of the β-AlFeSi is forced below the formation temperature of silicon eutectic, for this reason the Mg_2Si phase crystallize in metastable form. At low cooling rates, the decrease in temperature of β-AlFeSi is restricted, and the iron compound crystallized only as the β-phase. On the other hand the increase of cooling rate restricts the formation of the $FeAl_3$ and α-AlFeSi phases and increases the formation rate of the β-AlFeSi and Mg_2Si intermetallic phases.

Wear

The effect of porosity

The volume of porosity is effective on wear rate of Al6061 MMCs [23]. Investigations of the porosities in Al6061/Al_2O_3 MMCs have determined that interconnected porosities have not formed, and it was seen that the amount of porosities was decreased with pouring temperature and stirring speed. The porosity vol% increases as the viscosity of the semi-solid alloy increases due to larger volume fraction of particulates at lower pouring temperature. The upward movement of the air bubble becomes slow, as the liquid is more viscous [27]. In addition, the bubbles are attached to the particulates in the slurry and the force of buoyancy is counteracted. A similar trend in variation of porosity with pouring temperature is observed in Al6061/Al_2O_3 MMCs as shown in Fig. 2. From the Fig. 2, it is seen that the extent of porosity increase in Al6061/Al_2O_3 MMCs due to externally added Al_2O_3 particulates.

The porosity content changes with the process variables and the externally added particulate content [27]. The increase in stirring speed brought up an increase in porosity content up to an optimum level for each of these process variables. The particulate concentration also increases up to this level but beyond it both the porosity and particulate content reduce. Further, it has been observed that porosity content increased the distribution of inter particulate distance [30]. This result was thought to be due to a cluster of particulates attaching to an air bubble in the slurry. It was also observed that when the radius of the forced vortex region at the center exceeds the radius of the continuous region of a four-blade, stirrer vortex forms below the stirrer causing enhanced suction of particulates and air bubbles. These inferences of cold model experiment [34] seem logical to explain the variation of particulate and porosity content with the process variables.

The content of the particulates and matrix hardness are effective on wear rate of Al alloy MMCs [28]. In Fig. 3a and b, the effect of porosity on the wear rate and hardness are given, respectively for 200 m sliding distance and 100 N. The figures show that the amount of porosities decreased surface hardness and increased wear rate. The wear rate of Al alloy was affected directly by the porosity vol% however, the wear rate of Al_2O_3 reinforced composites were not affected from porosity vol% in a considerable amount. Moreover, the hardness of he Al alloy composites decreased with the increase in porosity vol%. This shows that the effect of Al_2O_3 addition on the wear resistance is higher than that of the porosity in the Al based MMCs.

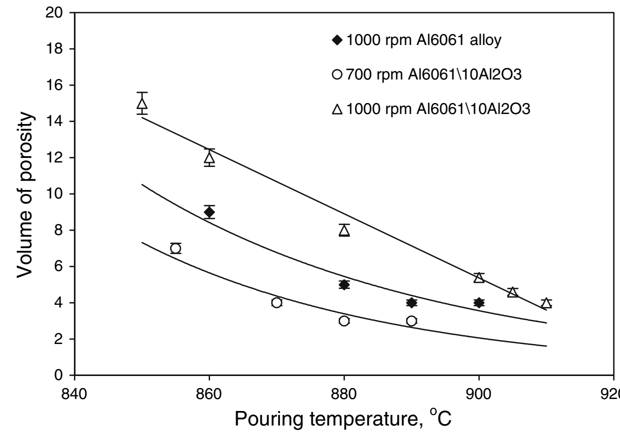

Fig. 2 The effect of pouring temperature on porosity content of Al6061 alloy and Al6061/10 vol% Al2O3 MMCs

The effect of microstructure

The wear rate versus sliding distance is plotted in Fig. 4 for unreinforced Al6061 alloy and Al6061 based MMC having 5–15 vol% Al_2O_3 particulates. The sample

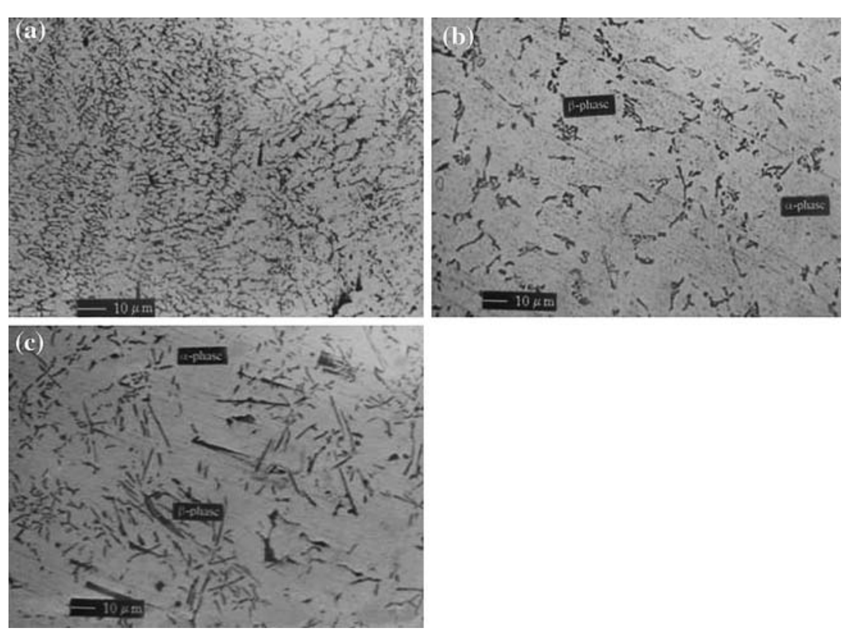

Fig. 1 (**a**) Primary-α crystals at low cooling rates(≈0.5 °C/s), (**b**) α- and β-phase in Al6061 alloy with intermediate cooling rate (≈10 °C/s), (**c**) α- and β-phase in Al6061/Al2O3 MMCs with high cooling rates (≈20 °C/s)

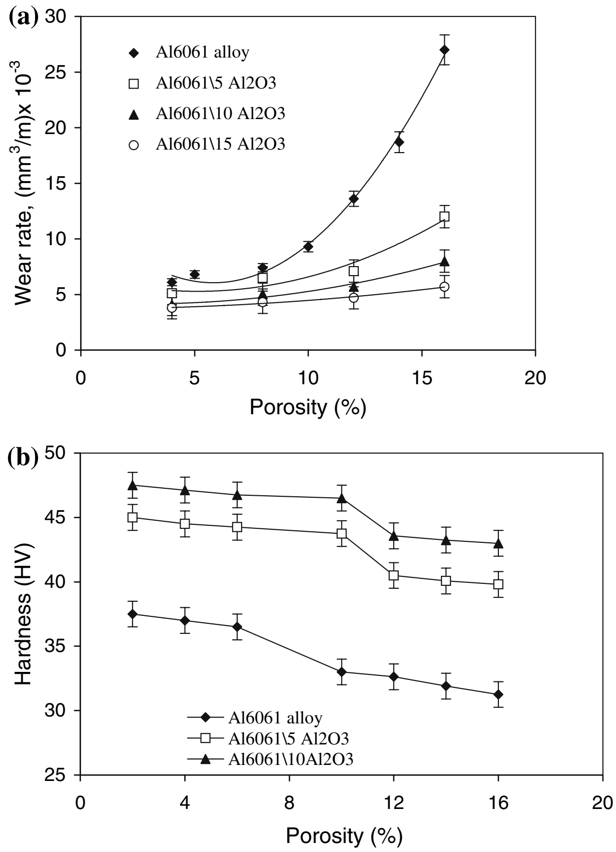

Fig. 3 (**a**) The effect of porosity on wear rate of Al6061 alloy and Al6061/Al2O3 MMCs at ambient temperature, (**b**) The effect of porosity on hardness of Al6061 alloy and Al6061/Al2O3 MMCs

worn against a DIN 5401 steel slider under 100 N. The wear rates of the composite did not increase linearly through the entire applied load range. The wear rate curves show that the change of wear volume with sliding distance is in the form of polynomial function. It was seen that, after a certain sliding distance and at constant velocity a transition to mild wear regime have been determined. Actually, this transition occurs when a critical temperature is reached at the contact surface, and this is observed when the critical temperature is reached at the contact surface because of frictional heating. From the beginning of the test, a steady state value of wear rate seemed to be attained for all materials after sliding 800 m, and the composite properties are still better than those of the Al alloys. These results showing the effect of Al_2O_3 particulates on wear resistance are again in agreement with some works [29], where it was reported that the addition of strong SiC, Al_2O_3 or TiC, particulates improved the wear resistance of Al, Fe or Cu based alloys if the particulates were well bonded to the matrix. As seen

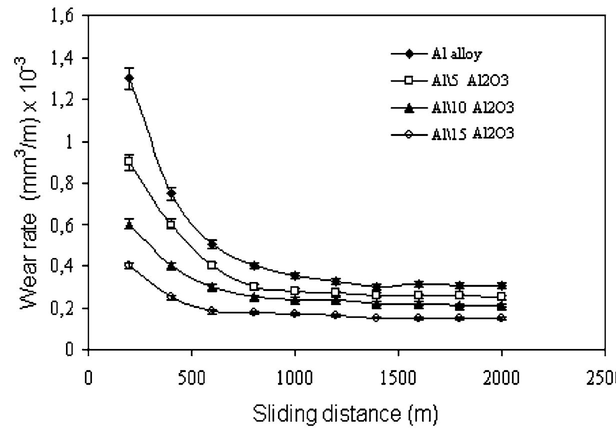

Fig. 4 The effect of sliding distance on wear rate of Al6061 alloy and Al6061/Al2O3 MMCs at ambient temperature

from Fig. 4 the alumina concentration decreased the steady state sliding distance. It is thought that the formation of β-AlFeSi and Mg_2Si intermetallic phases also affective on wear resistance.

Figure 5 compares the wear rates of Al6061 alloy and Al6061 based MMC having 5–15 vol% Al_2O_3 particulates at ambient temperature condition for 2,000 m sliding distance. The Fig. 5 shows that there is an intermediate load range, between 50 N and 80 N, where the wear resistances of composites and the unreinforced sample are similar. Unreinforced sample gave mild wear behavior between 80 N and 100 N loads and then it worn at severe wear behavior. The mild wear range were seen as 100–150, 150–250 and 200–300 N load, respectively for 5, 10 and 15 vol% Al_2O_3 particulate reinforced samples. In consequence, the increase of Al_2O_3 particulate vol% in the matrix and intermetallics delayed the transition of mild to severe wear and increased the transition loads. Addi-

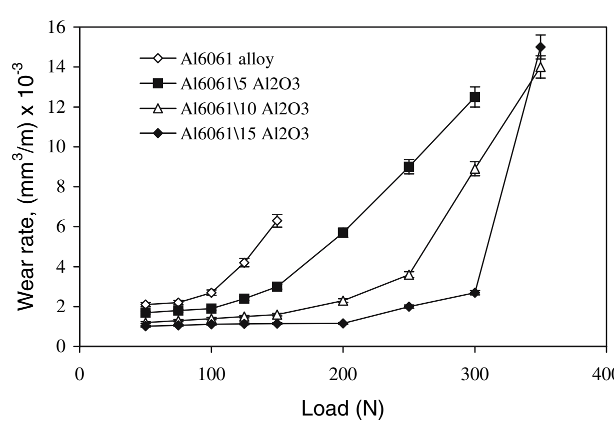

Fig. 5 The effect of load on wear rate of Al6061 alloy and Al6061/Al_2O_3 MMCs (Ambient temperature)

tionally, the dry sliding wear tests of the unreinforced Al6061 alloy and the Al6061/Al_2O_3 composites were performed in the temperature range of 273–475 K. The temperature was controlled by an external heat source. The friction coefficients and the wear rate of these materials were plotted in Fig. 6a and b, respectively, as function of the temperature. Figure 6a shows the effect of temperature on the friction coefficient of unreinforced Al alloy and Al6061/Al_2O_{3p} MMCs worn against a DIN 5401 steel slider under 100 N and for 2,000 m sliding distance. The friction coefficient of the Al6061/Al_2O_{3p} MMCs increased in a polynomial function through the entire temperature change. The friction coefficient curves shows that the friction coefficient (μ) obey a polynomial function. The wear rate curves reveals (Fig. 6b) that the wear rate (W) also obey a polynomial function as function of temperature. As given in Fig. 6a, the properties of Al6061/Al_2O_{3p} MMCs at the ambient temperature are maintained up to 350 K, where a sharp transition is found, and the friction coefficient increase and the wear resistance drops rapidly to the levels of the Al alloy over this temperature. Wear behavior of Al6061 alloy presents a smoother transition, although beyond 330 K the reduction in the wear resistance and the increase in the friction coefficient take place very rapidly. In the range of 330–370 K, the composite still shows an improvement over the Al6061 alloy, but beyond 440 K both materials showed a very similar wear behavior.

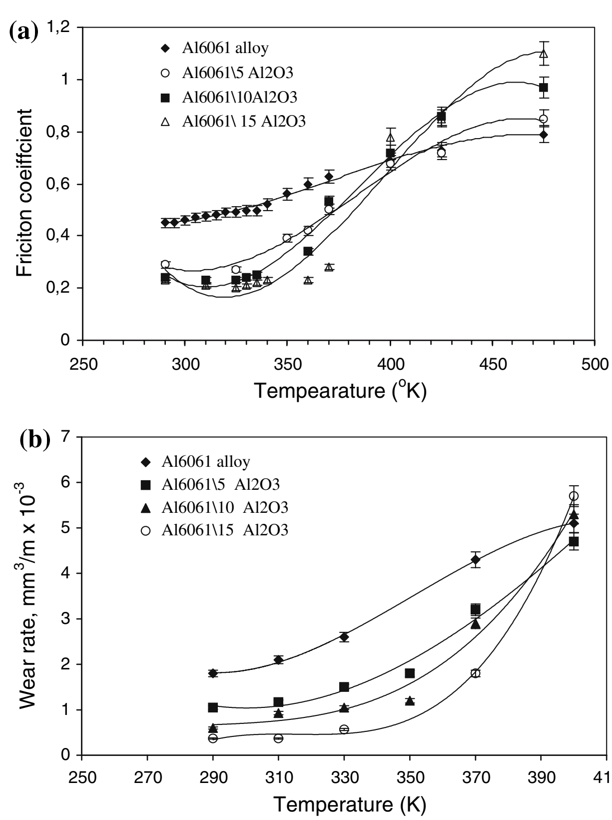

Fig. 6 (**a**) The effect of the temperature on the friction coefficient, (**b**) The effect of the temperature on wear rate under an external supplied heat (80 N)

Relationship between wear resistance, electrical resistivity and thermal conductivity

The relationship between electrical resistivity and Al_2O_3 vol% of the MMCs are given in Fig. 7. The electrical resistivity measurements were conducted by an external heat source, where the temperature was increased and the change of electrical resistivity for the samples were determined as function of temperature. The electrical resistivity of the samples increased by increasing Al_2O_{3p} concentration. It is known that heat absorbed from the materials increases the electrical resistivity and decreases wear resistance [33]. Hence, the thermal conductivities of the samples were calculated by using the electrical conductivity results.

$$\kappa = \frac{\pi^2}{3(k_B/e)^2}\sigma T = L\sigma T \tag{1}$$

where K is thermal conductivity, L is Lorentz constant (For Al alloys $L \approx 2,\ 20 \times 10^{-6}$ $W\Omega/K^2$) [30], T is temperature (K) and σ is electrical conductivity. In Fig. 8, the thermal conductivity of the samples in different concentration was given as a function of temperature. From the Fig. 8 it was deduced that, the effect of the Al_2O_3 particulates on the thermal conductivity changed as the function of temperature. In other words, as the temperature increased, the effect of the Al_2O_{3p} concentration on

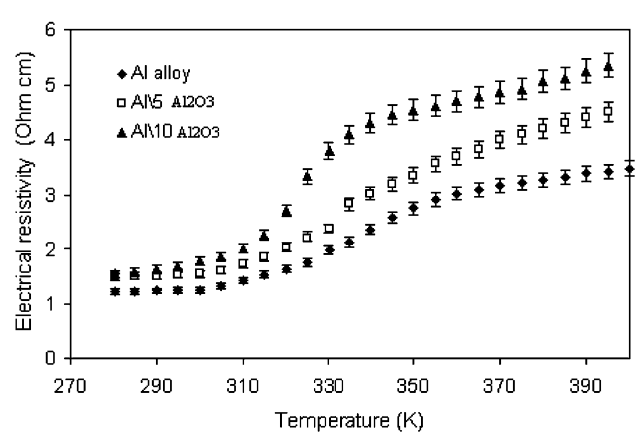

Fig. 7 The effect of the Al_2O_{3p} particulates on the electrical resistivity of Al\Al_2O_3 MMCs

the thermal conductivity increased up to a certain temperature level and after that a decrease in thermal conductivity values was detected. The thermal conductivity of the composite increased in a polynomial function through the entire temperature change. The heat conductivity curves shows that the heat conductivity (H) obeys a polynomial function. It is considered that the increase in transition temperature can be controlled by the mechanical properties of matrix. The thermal stability in the matrix provided by the presence of Al_2O_3 may be responsible for the higher transition temperature in the composites [31]. However, it should be noted that the local increase in temperature due to energy dissipation by friction could also influence this behavior [32]. Hence, the relationship between friction coefficient, electrical resistivity and thermal conductivity was taken into consideration. Room temperature measurements of the local heating due to friction of sliding surfaces showed an increase in the temperature of contact surface of Al6061 alloy approximately 280 K and 330 K temperature interval, depending on the applied load. In addition, the lower friction coefficient of Al6061\10% Al_2O_3 MMCs, which is in the temperature range of 280–370 K, may also be responsible for the better wear behavior up to 250 N loading. Hence, it was seen that Al_2O_3 reinforcement not only increases transition temperature of contact surface but also increases transition load.

The increase in electrical resistivity of the samples with addition of Al_2O_3 particulates can be attributed to electric and heat energy due to the increase of electron wave vibration. The temperature of sample increases with ascending of the vibrations at crystal structure and the free path, which the electrons would take decreases [33]. It was seen that with Al_2O_3 reinforcement the amount of collisions increased and the wave scattered, and the speed of net current flow decreased in a polynomial function. Some investigations [34] proposed that a transition from mild to severe wear would occur when the temperature between the contact surfaces exceeded a critical temperature. In this study, the surface temperatures of the Al6061 and Al6061/Al_2O_{3p} MMCs worn on steel slider were measured at different loads as a function of sliding distance. It was seen that the temperature of the contact surfaces increased with the sliding distance, until a thermal equilibrium was reached between contact surfaces. The unreinforced Al alloy sample shows a transition to severe wear at 80 N. Reinforcement of this alloy by alumina particulates improved the ability of the material to resist severe wear by increasing the transition load for 15 vol% Al_2O_3 to 285 N (Fig. 5). The results on particulate-reinforced aluminum–matrix composites showed that the transition to severe wear occurs when the temperature at the contact surface exceeds a critical temperature [35]. From the Fig. 9, it is detected that the temperatures of the subsurface regions increased with the applied load. For the unreinforced 6061Al, the severe wear obtained whenever the temperature reaches 400 K. According to some scientists [36], thermally activated deformation processes proceeds the severe wear for Al alloys after reaching this temperature range, and this softens the subsurfaces. It was seen in the Fig. 9 that before transition temperature the rate of the change for the temperature "Sa" was 0.25, however after the transition temperature the rate of the temperature change "Sb" increased to the 0.3. Zhang and Alpas considered that, the frictional heat generated during sliding is a function of

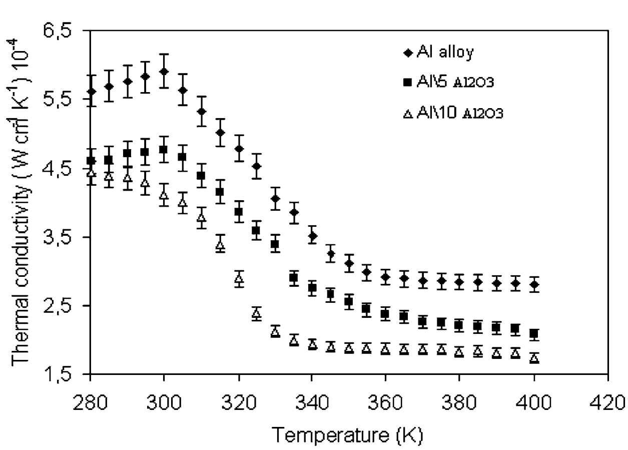

Fig. 8 The effect of the Al_2O_{3p} particulates on the thermal conductivity of Al\Al_2O_3 MMCs

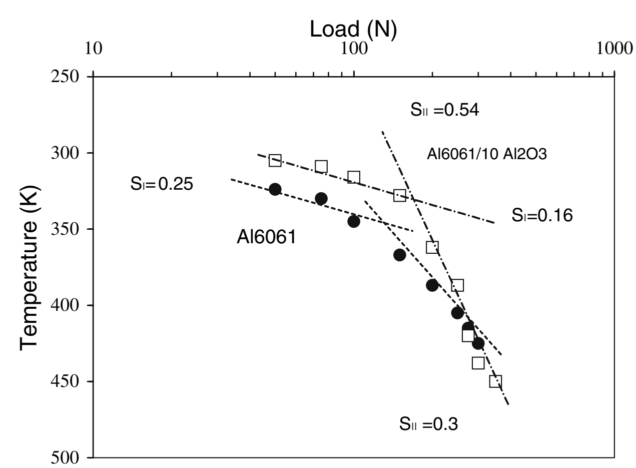

Fig. 9 The change of the contact surface temperatures of the worn surfaces of Al6061 alloy and Al6061/10 vol% Al_2O_3 MMCs after sliding to 1,000 m vs. load during dry sliding at ambient temperature. (S_I = Slope of temperature change before transition temperature, S_{II} = Slope of temperature change after transition temperature)

the applied load, sliding velocity, and the coefficient of friction [36]. The frictional heat generated at the interface diffuses away into the specimen and counterface materials. Therefore, a decrease in the coefficient of friction would result in a decrease in the interface temperature at a given load and sliding velocity. The Al6061/Al_2O_{3p} MMCs having a thermal conductivity lower than that of the Al6061 alloy restricts the rate of heat dissipation from the surface of the specimen; however MMCs have lower contact surface area, lower friction coefficient, and lower contact surface temperature. For this reason, the transition temperatures of MMCs are reached at higher degrees. On the other hand the rate of temperature change of Al6061/Al_2O_{3p} MMCs after transition temperature was detected as higher than Al6061 alloy (Sıı = 0.53). This was considered that after transition temperature a different and mixed type wear mechanisms proceeds for Al6061/Al_2O_{3p} MMCs. Nevertheless, it was clear that the reinforced composites with higher heat conductivity or lower friction coefficient increased the transition load from mild to severe wear. So that it can be say that the increase in Al_2O_{3p} particulate concentration decreases thermal conductivity values, but also decreases friction coefficient up to critical temperature. It is thought that the decrease of thermal conductivity with reinforcement amount decreases the effect of friction coefficient on wear rate. However, the critical temperature and load for mild to severe wear increases with the increase in Al_2O_3 amount. The relationship between thermal conductivity and friction coefficients is given in Fig. 10 at 290 K temperature. It is seen that both thermal conductivity and friction coefficients decrease in power expression with increase in particulate amount. As given below, the change of friction coefficient and thermal conductivity of the MMCs with alumina particulates is given as

$$\mu = xA^{-n} \tag{2}$$

$$K = xA^{-n} \tag{3}$$

where A is vol% Al_2O_3, μ is friction coefficient, K is thermal conductivity, n and x are constants. Depending on the change of thermal conductivity and friction coefficients with vol% alumina, it can be said that particulate reinforcements have increased thermal conductivity. In addition thermal conductivity and friction coefficients change in a very close relation. This means that alumina decreases friction resistance, on the other hand it also increases thermal resistance which is an unwanted property. Shortly, it is considered that to decrease contact temperature it is need to reduce the coefficient of friction or increase of thermal conductivity.

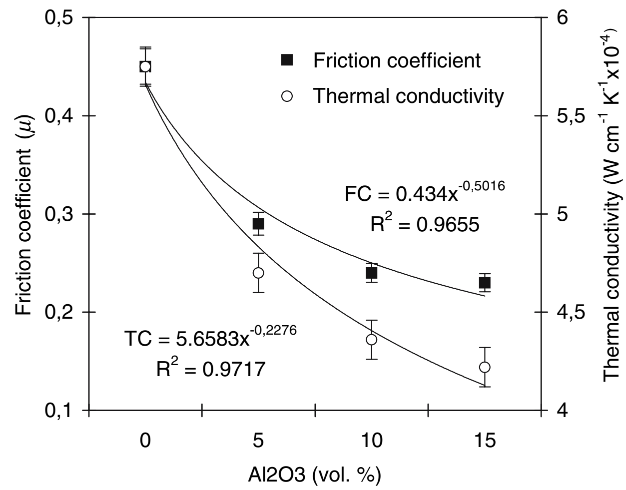

Fig. 10 The effect of Al_2O_{3p} particulates on the friction coefficient and the thermal conductivity at 290 K temperature

Conclusions

1. The crystallization behavior of the samples was studied before the reinforcement. It was aimed to detect the optimum microstructure before wear tests. The iron compounds crystallize in the β-phase by cooling from low temperatures, whereas from high temperatures, crystallization occurs in both α-phase and the β-phase. The externally added Al_2O_3 particulates behaved as nucleation site for β-Al–FeSi platelets.
2. The porosities in the structure increased wear rate. The wear rate of the Al alloy was significantly affected by the porosity while, the wear rate of the composite increased only slightly with increasing porosity.
3. The mild wear range for unreinforced Al6061 alloy, and 5, 10, 15% Al_2O_3 particulate reinforced Al6061/Al_2O_3 MMCs were seen as 100–150, 150–250 and 200–300 N load, respectively. The increase of Al_2O_3 vol% delayed the transition from mild to severe wear and increased the transition loads.
4. Friction coefficient and wear rate of the samples were changed with temperature in polynomial functions. The transition temperature for mild to severe wear of Al6061/Al_2O_3 MMCs increased with Al_2O_3 and intermetallic concentration.
5. The wear at high temperatures (400 K) was controlled by the matrix. The particulates were

fragmented near the sliding surface, and wear took place by subsurface delamination. The transition temperature was found to be 330 K for Al alloy, and 350–400 K interval for Al6061/Al_2O_3 MMCs. Rubbing the reinforced composites with higher heat conductivity or lower friction coefficient increased the transition load from mild to severe wear. On the other hand, the increase in Al_2O_{3p} particulate concentration decreased thermal conductivity, and increased friction coefficient. This result brought a critical temperature and load during mild to severe wear. Beyond this critical value, wear resistance of reinforced composites decreased.

References

1. Sangarakis N, Nunes J, Slepetz JM (1988) Eng Fract Mech 30:565
2. Ho TL, Peterson MB (1977) Wear 43:199
3. Toth IJ (1974) Composite material testing and design. ASTM STP 546, Philadelphia, PA, p 542
4. Lee JK, Earmme YV, Aronson HI, Russel KC (1980) Metall Trans A 11:1837
5. Flom Y, Arsenault RJ (1989) Acta Metall 37:2413
6. Christman T, Needleman A, Suresh S (1989) Acta Metall 37:3029
7. Bhanu Prasad VV, Prasad KS, Kuruvilla AK, Pandey AB, Bhat BVR, Mahajan YR (1991) J Mater Sci 26:460
8. Wu Y, Lavernia EJ (1992) In: Proc. Conf. advancements in synthesis and processes, Toronto, October 1992. Society for Advancement of Material and Process Engineering, p M692
9. Tiwari R, Herman H, Sampath S, Gudmundsson B (1991) Mater Sci Eng A 144:127
10. Milliere C, Suery M (1988) Mater Sci Technol 4:41
11. Mortensen A, Jin I (1992) Int Mater Rev 37(3):101
12. Delanny F, Froyen L, Deruyttere A (1987) J Mater Sci 22:1
13. Mcdanels DL (1985) Metal Trans 16A:1105
14. Ray S, Rohatgi PK (1972) Indian Patnet 12A:430
15. Mehrabian R, Flemings MC (1976) New trends in materials processing. ASM, Metals Park, p 98
16. Ghosh PK, Ray S, Rohatgi PK (1984) Trans Jpn Inst Met 25:440
17. Jha AK, Prasad SV, Upadhyaya GS (1989) Wear 133:163
18. Ghosh PK, Prasad PR, Ray S (1984) Z Metalkd 75:934
19. Ghosh PK, Ray S (1987) Communicated to Trans AM. Foundry men's Soc
20. Martines MA, Martin A, Llorca J (1993) Scripta Metall Mater 28:207
21. Singh J, Alpas AT (1996) Metall Mater Trans 27A:3135
22. Yilmaz O (2001) Mater Sci Tech 17:11
23. Yilmaz O, Buytoz S (2001) Comp Sci Tech 61–16:2381
24. Thomas G (1961–1962) J Inst Met 90:57
25. Backerud L, Chai G, Tamminen J (1990) Solidification Characterisation of Al Alloy, Vol. 2. AFS/Skan Aluminum, Oslo
26. Mortensen A, Cornie JA, Flemings MC (1988) J Metals 40:12
27. Axen N, Zum Gahr KH (1992) Wear 157:189
28. Prasad SV, Rohatgi PK (1987) J Metals 26:235
29. Yilmaz O, Aksoy M (2001) J Mater Proces Tech 249/10–11:902
30. Alpas AT, Zhang J (1992) Wear 83:155
31. Flom R, Arsenault J (1989) Acta Metall 37:2413
32. Lutts A (1961) Acta Met 9:577
33. Tjonng SC, Wang HZ, Wu SQ (1996) Meall Mater Trans 27A:2385
34. Alpas AT, Zhang J (1994) Metall Mater Trans A 25A:969
35. Zhang J, Alpas AT (1993) Mater Sci Eng A 160:25
36. Ashby MF, Abulawi J, Kong HS (1991) Tribol Trans 34:557